

Energy Loss Analysis of the Stationary Battery-supercapacitor Hybrid Energy Storage System

Yuyan Liu
School of Electrical Engineering
Beijing Jiaotong University
Beijing, China
18117014@bjtu.edu.cn

Zhongping Yang
School of Electrical Engineering
Beijing Jiaotong University
Beijing, China
zhpyang@bjtu.edu.cn

Fei Lin
School of Electrical Engineering
Beijing Jiaotong University
Beijing, China
flin@bjtu.edu.cn

Haofeng Yang
School of Electrical Engineering
Beijing Jiaotong University
Beijing, China
18121521@bjtu.edu.cn

Abstract—This paper proposes an energy loss analysis method for a stationary battery-supercapacitor hybrid energy storage system (HESS) in the case of regenerative braking energy recovery. Firstly, the energy loss model of stationary HESS is established. Then, the key parameters of the actual load are extracted to establish a simplified load model. The sensitivity analysis of energy loss is carried out by considering the influence factors such as voltage of substation, the state of charge for battery, and the characteristics of load profile. The simulation analysis of sensitive parameters are performed according to the actual conditions of Batong Line in Beijing .

Keywords—battery, supercapacitor, hybrid energy storage system, energy loss, sensitivity analysis

I. INTRODUCTION

Batteries and supercapacitors are commonly used energy storage devices. As the growing demand for the energy conservation and carbon emission decrease, energy storage technology used in urban rail transit has been more and more important. The characteristics of different ESS are different in power density and energy density[1]. The applications of batteries, supercapacitors and flywheels in urban rail transit are depicted in Fig. 1. In order to satisfy the functions of voltage compensation, recovery of regenerative braking energy and emergency traction, this paper chooses a stationary battery-supercapacitor hybrid energy storage system (HESS) in the substation to meet the above functions.

The research on the technology of ESS in urban rail transit mainly considers the impact of the traction power supply system. Paper [2] proposed a line-voltage control strategy to improve energy efficiency and reduce voltage drop of catenary. A voltage compensation control strategy of SC for a line with a long power supply distance was proposed in [3]. In [4], the control strategy of SC was proposed with the goal of maximizing the recovery of train braking kinetic energy. A control strategy to reduce catenary energy loss based on the SOC of SC was proposed in [5]. An online energy management controller effectively splits the load demand and achieves excellent result of the energy efficiency [6]. A controller of hybrid energy storage system was designed in [7], and the performances of the active hybrid power source in comparison to the passive one was discussed in [8]. Two real-time energy management strategies have been investigated for optimal current split between battery and

supercapacitor (SC) in electric vehicle applications [9]. However, there are relatively few studies considering the impact of the load side on the ESS. Paper [10] analyzed the effect of load on the efficiency and temperature rise of HESS based on electric vehicles. In [11], the energy loss of the battery semiactive HESS was analyzed based on the equivalent resistance and a pulsed current load. Paper [12] achieved a real-time HESS control strategy by optimizing current fluctuations of battery and energy utilization of SC. Most of these studies considering characteristics of ESS are based on electric vehicles. This paper will analyze the impact of the braking situation on the HESS in the urban rail traction power supply system. The sensitivity analysis of the energy loss will provide the basis for the analysis of the characteristics of the HESS side for the research of other stationary HESS.

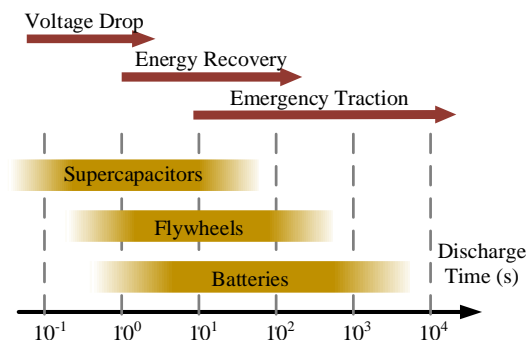


Fig. 1. Application of ESS in urban rail transit

The focus of this discussion is on establishing a guideline for evaluating and improving management strategies of the HESS. The proposed hybrid energy storage energy loss model is described in section II. Section III analyzes the load characteristics of train operation and proposes a simplified load model. And then sensitivity analysis of hybrid energy storage energy loss is described. Effect of sensitive parameters on energy loss is discussed in Section IV. Section V is the conclusion.

II. MODEL OF HESS

A. System Configuration

In order to ensure the safety and reliability of the stationary HESS, the HESS topology model of Fig. 2 is adopted. The

battery and SC are connected in parallel with the substation via dc-dc converters 1, 2, respectively. The characteristic of substation is simulated by an ideal voltage source in series with the resistance. Using series diodes to represent the uncontrolled rectification characteristic of traction substation. To simplify the load model, an ideal current source is used here instead of the load of traction power system. When the load current i_l is negative, the regenerative braking energy is recovered by the HESS.

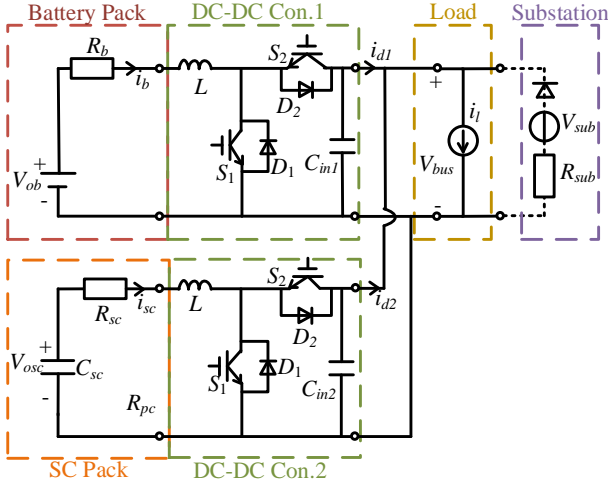


Fig. 2. The structure topology of HESS

B. Energy Loss Model

The energy loss of HESS mainly comes from battery, SC and two dc-dc converters. The energy loss of each part is discussed below.

1) *Battery Pack*: Considering the load frequency characteristic of urban rail transit and the nonlinear characteristic of the battery, this paper uses a first-order equivalent circuit model with a controlled voltage source and an equivalent resistance in series to model the battery. V_{ob} is equivalent to the open circuit voltage of the battery, and R_b is the internal resistance of the battery. V_{ob} and R_b are related to the SOC of the battery[13], Fig. 3 shows the relationship between parameters of the battery cell and the SOC used in the simulation, V_{ob} and R_b are expressed as sixth-order polynomials as

$$V_{ob} = a_0 + a_1 \times SOC_b + a_2 \times SOC_b^2 + a_3 \times SOC_b^3 + a_4 \times SOC_b^4 + a_5 \times SOC_b^5 + a_6 \times SOC_b^6 \quad (1)$$

$$R_b = b_0 + b_1 \times SOC_b + b_2 \times SOC_b^2 + b_3 \times SOC_b^3 + b_4 \times SOC_b^4 + b_5 \times SOC_b^5 + b_6 \times SOC_b^6 \quad (2)$$

where SOC_b is a specific SOC of the battery.

The energy loss of the battery is expressed as

$$P_{LOSS_BAT} = i_b^2 R_b \quad (3)$$

where i_b is the battery current. Refer to (3), the energy loss of the battery is mainly affected by i_b . Since i_b is converted by a dc-dc converter, it is related to the parameter of DC bus. i_b is expressed as

$$i_b = \frac{V_{ob}}{2R_b} - \frac{\sqrt{V_{ob}^2 - 4R_b V_{bus} i_{d1} \eta_1}}{2R_b} \quad (4)$$

$$\eta_1 = \frac{(V_{ob} - i_b R_b) |i_b|}{(V_{ob} - i_b R_b) |i_b| + P_{LOSS_DD1}} \quad (5)$$

where V_{bus} is the voltage of substation; η_1 is the efficiency of dc-dc converter 1. η_1 is expressed as (5). The efficiency maps for Buck mode of dc-dc converter 1 is demonstrated in Fig. 4. In Fig.4, the battery SOC value range is from 0.4 to 0.8 and the battery current varies from 160 to 200A. It can be observed that the dc-dc converter has lower efficiency because of a light load. To simplify the calculation, assume that the efficiency is constant.

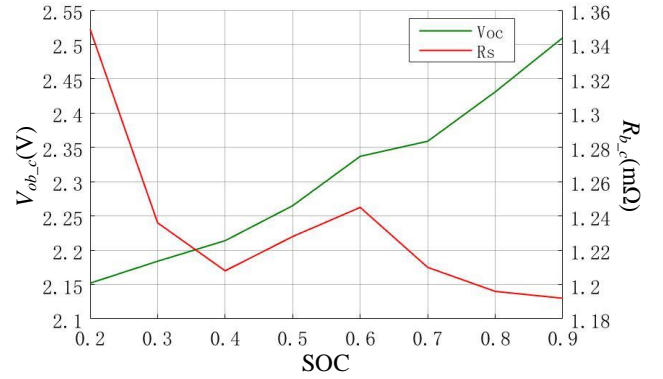


Fig. 3. The relationship between battery cell voltage, internal resistance and SOC

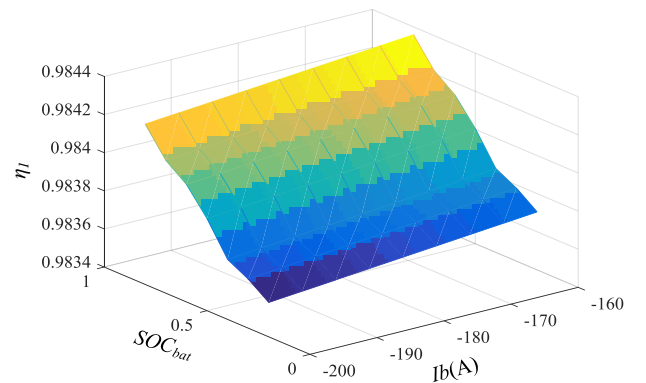


Fig. 4. Efficiency map of dc-dc converter 1 in Buck mode.

2) *SC Pack*: This discussion uses a first-order equivalent circuit model to describe the SC. V_{osc} is equivalent to the open circuit voltage of the SC, R_{sc} is the internal resistance of the SC. The energy loss of the SC is approximately expressed as

$$P_{LOSS_SC} = i_{sc}^2 R_{sc} \quad (6)$$

where i_{sc} is the SC current. i_{sc} is expressed as

$$i_{sc} = \frac{V_{sc}}{2R_{sc}} - \frac{\sqrt{V_{sc}^2 - 4R_{sc}V_{bus}i_{d2}\eta_2}}{2R_{sc}} \quad (7)$$

$$\eta_2 = \frac{(V_{sc} - i_{sc}R_{sc})|i_{sc}|}{(V_{sc} - i_{sc}R_{sc})|i_{sc}| + P_{LOSS_DD2}} \quad (8)$$

where η_2 is the efficiency of dc-dc converter 2. η_2 is expressed as (8). The efficiency maps for Buck mode of dc-dc converter 2 is demonstrated in Fig. 5. In Fig. 5, the SC current value range is from 800 A to 1000 A and the SC voltage varies from 336 V to 744 V. It can be observed that the efficiency of the dc-dc converter 2 is much lower than that of the dc-dc converter 1 because of a larger current.

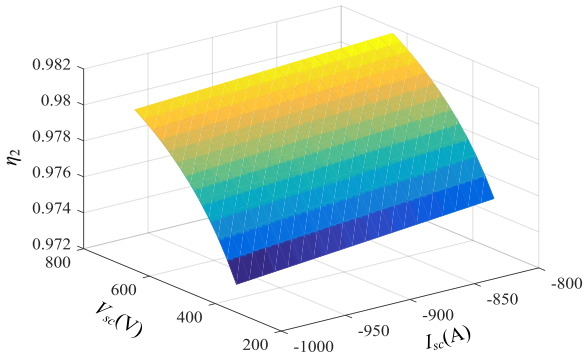


Fig. 5. Efficiency map of dc-dc converter 2 in Buck mode.

3) DC-DC converter: The energy loss of dc-dc converter are mainly from series inductors, IGBTs and anti-parallel diodes. Since the paper only considers the HESS energy loss when i_l is negative, only the dc-dc energy loss in the buck mode is modeled. The energy loss of IGBT is mainly composed of switching loss and conduction loss. The switching loss P_{sLoss_DD} generated by the IGBT is expressed as

$$\begin{cases} E_{on_DD} = C_{on} V_{real} I_{real} \\ E_{off_DD} = C_{off} V_{real} I_{real} \end{cases} \quad (9)$$

$$\begin{aligned} P_{sLoss_DD} &= f_s (E_{on_DD} + E_{off_DD}) \\ &= f_s V_{real} I_{real} (C_{on} + C_{off}) \end{aligned} \quad (10)$$

where C_{on} and C_{off} are the switching loss parameters calculated by the IGBT data specification, respectively; V_{real} is the voltage across the IGBT and I_{real} is the current flowing through the IGBT. f_s is the switching frequency.

At steady state, the IGBT and the anti-parallel diode have a conduction voltage drop with a conduction current. The expression of the conduction loss is

$$\begin{aligned} P_{CLOSS_DD} &= i_L^2 R_L + (i_L^2 R_D + i_L V_D)(1-d_s) \\ &\quad + (i_L^2 R_s + i_L V_s)d_s \end{aligned} \quad (11)$$

where i_L is the current of the inductance; R_L is the equivalent series resistance of the inductance; R_s and V_s are the on-resistance and equivalent voltage drop of the converter respectively; R_D and V_D are the on-resistance and equivalent voltage drop of the diode D, respectively; the switch duty ratio d_s is expressed as

$$d_{s1} = (V_{ob} - i_b R_b) / V_{bus} \quad (12)$$

$$d_{s2} = (V_{sc} - i_{sc} R_{sc}) / V_{bus} \quad (13)$$

So the energy loss of the converter can be expressed as

$$P_{LOSS_DD} = P_{CLOSS_DD} + P_{sLoss_DD} \quad (14)$$

III. SENSITIVITY ANALYSIS

A. The Characteristic of the Load

HESS mainly plays the role of compensating the catenary voltage and recovering the regenerative braking energy during the normal operation of the traction power supply system. Regenerative braking energy is generated when the train decelerates. In order to absorb the regenerative braking energy, the Batong line in Beijing is equipped with a hybrid energy storage system of 200kW battery and 800kW SC. The regenerative braking power is analyzed by taking the operating conditions of the train from Tuqiao Station to Guoyuan Station as an example. The train running process is expressed as

$$\begin{cases} \dot{s} = v \\ M\dot{v} = u_f \cdot F_{tr}(v) - u_b \cdot F_{br}(v) - R(v) \\ \quad - F_{grad}(s) - F_{cu}(s) \\ v(0) = 0, s(0) = 0 \\ v(T) = 0, s(T) = S_i \end{cases} \quad (15)$$

The train is generally operated with 4 level of traction and 3 level of braking in normal operation. The running curve is shown in Fig. 6. It can be seen from Fig. 6 that the maximum braking power of the train does not exceed 1 MW. And the train braking time is about 20~40s. When the braking power exceeds 800kW, in order to absorb the maximum regenerative braking power, assuming at least one device in the battery and the SC needs to operate at full power. Therefore, in the energy consumption analysis, the regenerative braking power below 800kW and above 800kW are analyzed separately. Regenerative braking power above 800kW is discussed in Section IV.

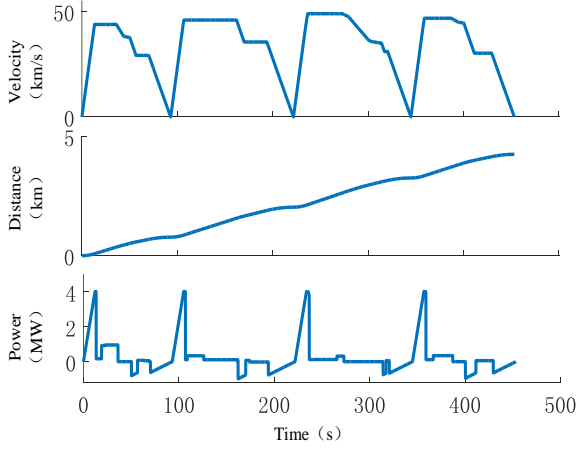


Fig. 6. Train operation curve

For theoretical analysis, the pulsed power profile is used to represent the load in combination with the actual braking situation [14]. As shown in Fig. 7, the pulsed load power P_{load} is the regenerative braking power that needs to be absorbed by the HESS, and T is the regenerative braking time. So, the load current

$$i_t = P_{load} / V_{bus} \quad (16)$$

When the charging power of battery is P_{BAT} , the SC charging power is expressed as

$$P_{SC} = P_{load} - P_{BAT} \quad (17)$$

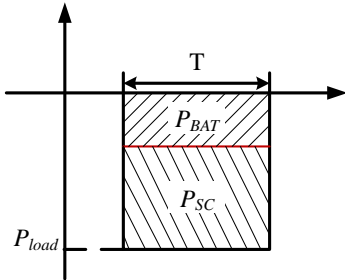


Fig. 7. The pulsed load power

B. Sensitivity Analysis Result

Before doing sensitivity analysis, the following assumptions were made:

- The charging power of the HESS is nearly constant.
- The voltage of DC bus is a constant.

The global sensitivity analysis is mainly to analyze the effects of load, energy storage system parameters, and bus voltage on the energy loss of the HESS. This paper uses the Sobol' indices sensitivity analysis method. This method is used to quantify the effect of each parameter or related parameter on the variation of the output results [15]. This discussion mainly

analyzes the impact of P_{load} , P_{BAT} , SOC_{b_init} and V_{bus} on energy loss of the HESS. In order to meet the voltage requirements, the battery cells are connected in 23S2P and the SC modules are connected in 14S8P. The range of variation of P_{load} , P_{BAT} , SOC_{b_init} and V_{bus} is shown in TABLE I. . This discussion is mainly for braking conditions, so the bus voltage is larger than the 836V which is no-load voltage of the substation. This discussion uses the quasi-Monte Carlo algorithm to extract 800,000 Halton points to evaluate first-order sobol indices. The expectation and standard deviation of the effects of 800,000 samples on the battery and its parallel dc-dc converter section, SC and its parallel dc-dc converter section, and the overall energy loss of HESS, $E(y)$ and $\sigma(y)$, are shown in TABLE II. . It can be seen that the energy loss of the SC in the HESS is slightly higher than that of the battery; meanwhile, the energy loss of the SC is relatively more sensitive to the battery.

TABLE I. RANGE OF SENSITIVE VARIABLES

Parameter	P_{load}	P_{BAT}	SOC_{b_init}	V_{bus}
Min	200kW	50kW	0.4	860V
Max	800kW	200kW	0.8	900V

TABLE II. THE EXPECTATION AND STANDARD OF ENERGY LOSS

	Battery	SC	HESS
$E(y)$	0.12	0.38	0.5
$\sigma(y)$	0.13	0.44	0.43

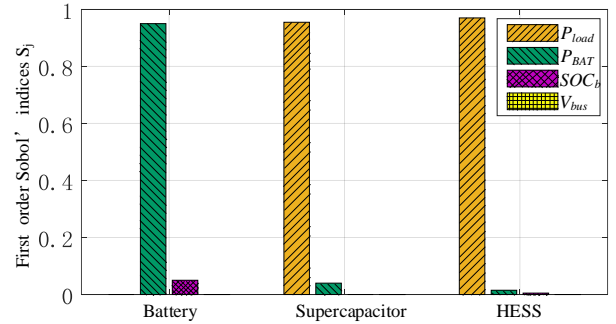


Fig. 8. First order Sobol' indices for energy loss in battery.

It can be seen from the first-order Sobol' indices of Fig. 8 that the DC bus voltage has slight effect on the energy loss of the energy storage system. The energy loss of the battery is affected by the two variables of P_{BAT} and SOC_b . The energy loss of the SC is mainly affected by the load.

IV. INFLUENCE OF HESS PARAMETERS

As can be seen from the above sensitivity analysis, the battery energy loss is mainly related to its initial SOC and charging power; and the SC energy loss is primarily related to the overall power distribution. From the above sensitivity analysis, the bus voltage hardly affects the energy loss of the HESS. Therefore, when analyzing the energy loss, the bus voltage is assumed to be a constant value for analysis. The actual impact of these sensitive factors on HESS will be discussed below.

A. Impact of Sensitive Parameters

In the case that the load power P_{load} is 600kW and T is 20s, the energy loss of the battery and dc-dc converter 1 varies with P_{BAT} and SOC_{b_init} are shown in Fig. 9 and Fig. 10, respectively. As SOC_{b_init} increases, the energy loss of the battery and dc-dc converter all decrease.

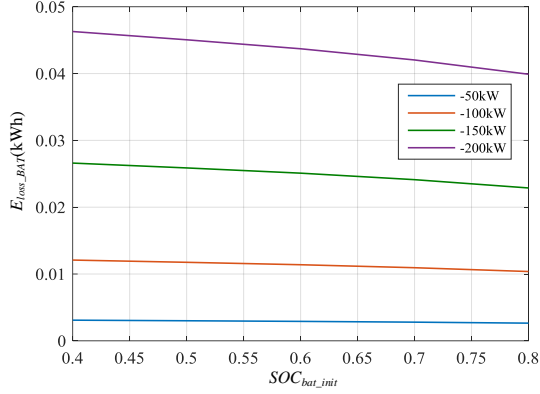


Fig. 9. Relationship between battery energy loss and sensitive parameters.

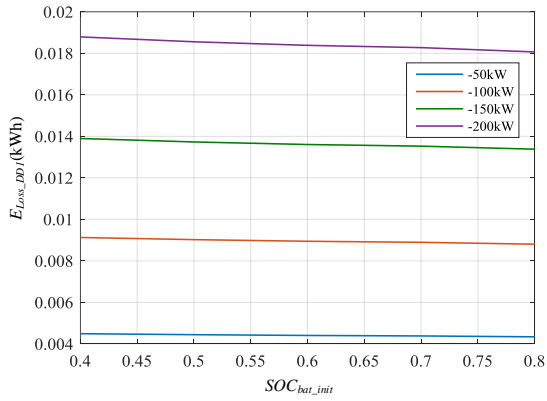


Fig. 10. Relationship between dc-dc converter1 loss and sensitive parameters

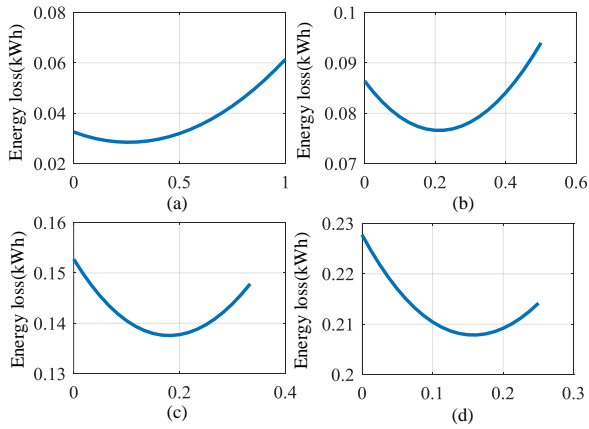


Fig. 11. Energy loss with different C_d . (a) $P_{load}=-200kW$, (b) $P_{load}=-400kW$, (c) $P_{load}=-600kW$, (d) $P_{load}=-800kW$

Under the premise that the initial SOC of the battery is 0.4 and the V_{bus} is 860V, the allocated power of the battery is changed, and the energy loss of the HESS is as shown in Fig.11. The power allocation ratio C_d is expressed as

$$C_d = \frac{P_{BAT}}{P_{load}} \quad (14)$$

The four subgraphs of Fig. 11 show the trend of energy loss under different P_{load} . The energy loss of HESS decreases first and then increases with the increase of C_d . As the load power increases, the P_{BAT} corresponding to the lowest energy loss increases. Take the load power of 600kW as an example. At this time, the lowest energy loss corresponds to P_{BAT} of 120kW. The dc-dc converter is controlled by the voltage and current double closed loop, and the charge threshold is set to 860V. The simulation results are shown in Fig. 12 and Fig. 13. It can be seen when the load power is 600 kW, the battery and the SC start to charge, and the DC bus voltage is stabilized at 860 V; the voltage of the SC rises rapidly. Since the battery is charged with constant power and P_{load} is a constant, the SC current rises in order to maintain a constant charging power.

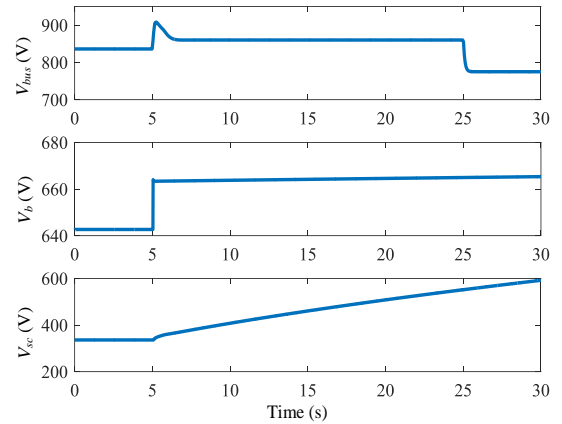


Fig. 12. Voltages of the dc bus, battery and supercapacitor packs

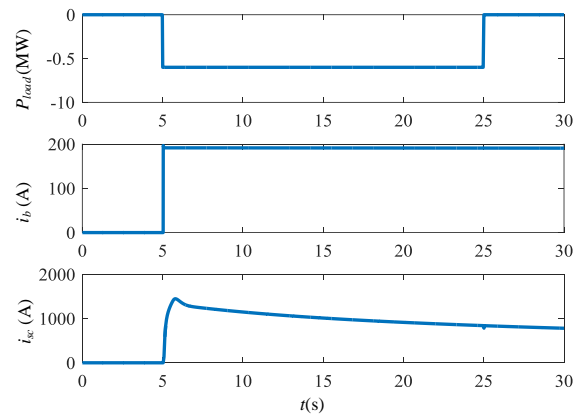


Fig. 13. Current of the battery packs, the supercapacitor packs and the catenary.

B. Impact of P_{load} above 800kW

If P_{load} is larger than 800kW, assuming at least one ESS need to charge with full power. The variation of HESS energy loss is discussed below for the load power in the range of 800kW to 1MW.

The HESS energy loss when the battery and the SC are prefer charged at full power, respectively, is shown in Fig. 14. When P_{load} is lower than 800kW, the energy loss of the battery priority full power charge is less than that of the SC. When the P_{load} exceeds 800kW, the energy loss of the SC priority full power charge is less than the battery priority.

When the SC is fully charged, the relationship between the HESS energy loss and the initial SOC of the battery is shown in Fig. 15. As can be seen from Fig. 15, when the SC is fully charged, the energy loss of the battery decreases as the initial SOC increases. In order to reduce the battery energy consumption when controlling HESS, the SOC_{b_init} should be large as much as possible while satisfying the recovery of regenerative braking energy.

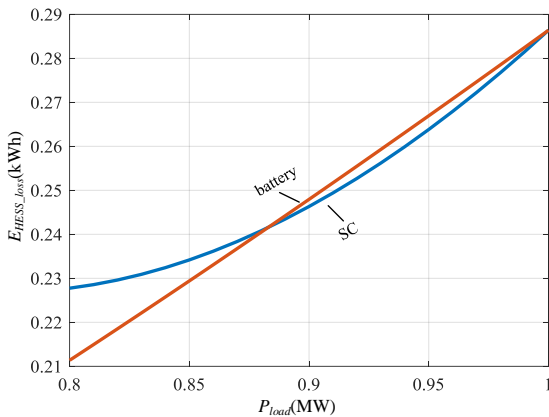


Fig. 14. Energy loss for battery full power charging and SC full power charging

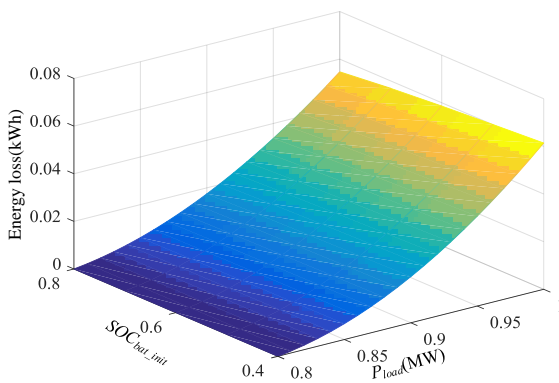


Fig. 15. Energy loss of battery and dc-dc converter1 for SC full power charging

V. CONCLUSION

In this paper the energy loss of stationary HESS is analyzed. The paper first established the HESS energy loss model. The

first-order Sobol' indices were used to analyze the sensitivity of the parameters affecting the energy loss in hybrid energy storage system. It can be seen from the analysis that the magnitude of the bus voltage hardly affects the of the battery are sensitivity variables for energy loss. Then, the trend of the sensitivity parameter to the energy loss was also quantitatively analyzed. Under different loads, the power distribution ratio C_d at the lowest point of energy loss is different. As the load power increases, the battery distribution power corresponding to the lowest energy loss point is higher. In the actual operation process, in order to reduce the energy loss of the HESS, the appropriate power distribution ratio should be selected.

REFERENCES

- [1] G. Graber, V. Calderaro, V. Galdi, A. Piccolo, R. Lamedica and A. Ruvio, "Techno-economic Sizing of Auxiliary-Battery-Based Substations in DC Railway Systems," in *IEEE Transactions on Transportation Electrification*, vol. 4, no. 2, pp. 616-625, June 2018.
- [2] F. Ciccarelli, D. Iannuzzi, K. Kondo, and L. Fratelli, "Line-Voltage Control Based on Wayside Energy Storage Systems for Tramway Networks," *IEEE Transactions on Power Electronics*, vol. 31, no. 1, pp. 884-899, Jan 2016.
- [3] Rufer, A., et al, "A supercapacitor-based energy storage substation for voltage compensation in weak transportation networks," *IEEE Transactions on Power Delivery*, vol. 19, no. 2, pp. 629-636, 2004.
- [4] Ciccarelli, F., et al., "Improvement of Energy Efficiency in Light Railway Vehicles Based on Power Management Control of Wayside Lithium-Ion Capacitor Storage," *IEEE Transactions on Power Electronics*, vol. 29, no. 1, pp. 275-286, 2014
- [5] Barrero, R., X. Tackoen, and J. Van Mierlo. "Stationary or onboard energy storage systems for energy consumption reduction in a metro network." *Proceedings of the Institution of Mechanical Engineers, Part F: Journal of Rail and Rapid Transit* 224.3(2010):207-225.
- [6] Shen, J. Y. and A. Khaligh, "A Supervisory Energy Management Control Strategy in a Battery/Ultracapacitor Hybrid Energy Storage System," *IEEE Transactions on Transportation Electrification*, vol. 1, no. 3, pp. 223-231, 2015
- [7] Gao, L. J., et al., "Power enhancement of an actively controlled battery/ultracapacitor hybrid," *IEEE Transactions on Power Electronics*, vol. 20, no. 1, pp. 236-243, 2005
- [8] Zhao, C., et al., "Quantitative Efficiency and Temperature Analysis of Battery-Ultracapacitor Hybrid Energy Storage Systems," *IEEE Transactions on Sustainable Energy*, vol. 7, no. 4, pp. 1791-1802, 2016
- [9] Shen, J. Y. and A. Khaligh, "Design and Real-Time Controller Implementation for a Battery-Ultracapacitor Hybrid Energy Storage System," *IEEE Transactions on Industrial Informatics*, vol. 12, no. 5, pp. 1910-1918, 2016
- [10] Zhao, C., et al., "Equivalent Series Resistance-Based Energy Loss Analysis of a Battery Semiactive Hybrid Energy Storage System," *IEEE Transactions on Energy Conversion*, vol. 30, no. 3, pp. 1081-1091, 2015
- [11] Yin, H., et al., "Utility Function-Based Real-Time Control of A Battery-Ultracapacitor Hybrid Energy System," *IEEE Transactions on Industrial Informatics*, vol. 11, no. 1, pp. 220-231, 2015
- [12] Cao, Y., et al., "Multi-timescale Parametric Electrical Battery Model for Use in Dynamic Electric Vehicle Simulations," *IEEE Transactions on Transportation Electrification*, vol. 2, no. 4, pp. 432-442, 2016
- [13] Chen, M. and G. A. Rincon-Mora, "Accurate electrical battery model capable of predicting, runtime and I-V performance," *IEEE Transactions on Energy Conversion*, vol. 21, no. 2, pp. 504-511, 2006
- [14] Kuperman, A. and I. Aharon, "Battery-ultracapacitor hybrids for pulsed current loads: A review," *Renewable & Sustainable Energy Reviews*, vol. 15, no. 2, pp. 981-992, 2011
- [15] Sobol, I. M., "Global sensitivity indices for nonlinear mathematical models and their Monte Carlo estimates," *Mathematics and Computers in Simulation*, vol. 55, no. 1-3, pp. 271-280, 2000